Fast Closure of N-Terminal Long Loops but Slow Formation of β Strands Precedes the Folding Transition State of Escherichia coli Adenylate Kinase

ARTICLE *in* BIOCHEMISTRY · MAY 2014

Impact Factor: 3.02 · DOI: 10.1021/bi500069w · Source: PubMed

BIOCHEMISTRY
including biophysical chemistry & molecular biology

Article

pubs.acs.org/biochemistry

Fast Closure of N-Terminal Long Loops but Slow Formation of β Strands Precedes the Folding Transition State of *Escherichia coli* Adenylate Kinase

Tomer Orevi, Eldad Ben Ishay, Sivan Levin Gershanov, Mayan Ben Dalak, Dan Amir, and Elisha Haas*

The Goodman Faculty of Life Sciences, Bar Ilan University, Ramat Gan, Israel 52900

Supporting Information

ABSTRACT: The nature of the earliest steps of the initiation of the folding pathway of globular proteins is still controversial. To elucidate the role of early closure of long loop structures in the folding transition, we studied the folding kinetics of subdomain structures in *Escherichia coli* adenylate kinase (AK) using Förster type resonance excitation energy transfer (FRET)-based methods. The overall folding rate of the AK molecule and of several segments that form native β strands is 0.5 ± 0.3 s^{-1}, in sharp contrast to the 1000-fold faster closure of three long loop structures in the CORE domain. A FRET-based "double kinetics" analysis revealed complex transient changes in the initially closed N-terminal loop structure that then opens and closes again at the end of the folding pathway. The study of subdomain folding *in situ* suggests a hierarchic ordered folding mechanism, in which early and rapid cross-linking by hydrophobic loop closure provides structural stabilization at the initiation of the folding pathway.

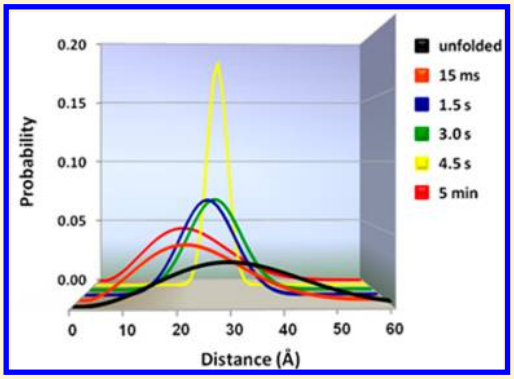

Identifying the key interactions that lead the fast protein folding transition via the early reduction of chain entropy is critical to the mechanistic understanding of the folding process.[1,2] Compaction (collapse) detected by FRET-based methods is the first folding event to occur, even in the intermediate free refolding of two-state folders.[3,4] Chain collapse is a solvent-induced nonspecific response to a change in system conditions (common to any polymer molecule),[5] yet fast formation of specific interactions might lead to early intermediates that already contain specific loose subdomain structures.[6−8] In particular, nonlocal interactions can be very effective in reducing the conformational space occupied by the ensemble, which is still mostly disordered. Therefore, much effort has been focused on characterization of the transient subdomain structures formed early in the folding transition. Such structures induce constraints upon the random search for specific intramolecular interactions and, thus, guide the folding chain toward productive routes, prior to the rate-limiting step of folding. Major progress was made in studies of the structures of the transition state ensembles (TSE), which in many cases include the main features of the native topology of the chain fold.[9−11]

When considering possible mechanisms of stepwise structure formation in the folding transition, the "bottom-up" model seems to be the most intuitive.[12,13] In this mechanism, local interactions (LIs) between near neighbor residues along the chain are assumed to form first and stabilize short structural elements, such as secondary structures. Those elements then coalesce to form higher-level contacts. The alternative mechanism assumes that the less probable nonlocal interactions (NLI) between monomers separated by 10 or more residues along the chain are an essential component of the initial folding steps. The relative importance of local versus nonlocal interactions in directing the mechanism of folding has been investigated for many years, mainly by means of simulations and theoretical arguments.[14−18] Most studies concluded that the initial steps of the folding mechanism are dominated by LIs, while the nonlocal ones provide nonspecific stabilization of the compact conformers[19−24] and the folding nucleus.[25,26] The question of whether LIs or NLIs are more important or dominant in the initiation of folding or for determination of the direction and rate of the folding transition remains unanswered.

In 1995,[27] we proposed that closure of a small number of long loop segments by NLIs between clusters of mostly nonpolar residues at their ends occurs as part of the initiation of the folding transition.[28] In the context presented here, we refer to loops that are longer than the Ω-loops that are thought to be short ($n \leq 16$).[29] In that "closed long loops" hypothesis, we assumed that the NLIs that close the loops do not depend on the secondary structures of the interacting clusters. Furthermore, this model proposes that the early closed loops sufficiently restrict the conformational space and form ensembles of conformations that then proceed to the TSE and the folded ensembles.[30]

In this study, we applied trFRET-based methods in an attempt to trace the time course of closure of long loops and

Received: January 20, 2014
Revised: May 2, 2014
Published: May 2, 2014

dx.doi.org/10.1021/bi500069w | *Biochemistry* 2014, 53, 3169−3178

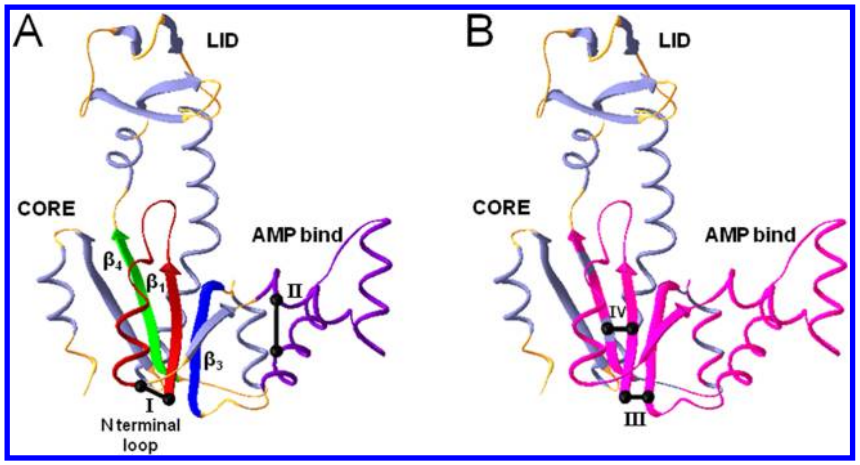

Figure 1. Ribbon diagram of the *E. coli* adenylate kinase highlighting the labeled chain segments and the subdomain structures that were labeled and monitored by the FRET experiments. (A) Structure of the ligand free AK molecule (PDB entry 4AKE) in which structural elements are highlighted. The N-terminal loop (loop I, residues 1−26) is colored red. β strands that were labeled are colored. Strand β_1 is included in loop I (residues 1−6, red). Strands β_3 (residues 79−85, blue) and β_4 (residues 104−110, green) form native interactions with β_1 in the native structure. (B) Merged loop structure: loop III (residues 1−86, magenta), which includes loops I and II and strands β_1 and β_3; and loop IV (residues 1−111, magenta dashed), which includes loops I−III. Loop IV is closed by the segments forming strands β_1 and β_4. The pairs of black dots represent the interacting hydrophobic clusters of residues located at the nodes of the labeled loops, and the connecting lines represent the native close contacts between those clusters. All the elements that were studied are located in the CORE domain of AK.

the formation of β strands in the CORE domain, during the refolding transition of adenylate kinase (AK) from *Escherichia coli* (Figure 1). This was done to test the hypothesis that a small number of long loops form early in the folding transition, even prior to the formation of secondary structure elements.[28,31] The trFRET-based "double kinetics" method[32−34] was developed for the detection of transient intramolecular distance distributions in the fast collapsed state of globular proteins and during the full folding transition.[35−37] AK is a 214-residue single-chain, three-domain protein that catalyzes the transfer of a phosphoryl group between ATP and AMP. The native topology of the CORE domain of AK is defined by seven long loops. The residues at opposite termini of each loop segment form a strong hydrophobic node, as judged by the number of contacts between them. In the past, we have found that the long loop enclosing the whole AMP_{bind} domain is closed within the mixing dead time of the double kinetics device.[37] In this study, we wished to trace the course of structure formation in selected segments of the protein backbone. Six representative structural elements were studied. We show here that loop structure elements were already formed within the dead time of the mixing device (1 ms), but at that time, the β strands tested had not yet reached their native conformation.

MATERIALS AND METHODS

Sample Preparation and Labeling. *E. coli* AK mutants were constructed by site-directed mutagenesis, overexpressed, and purified, as described previously.[37,38] All variants were derived from a cysteine free C77S AK gene. Donor only mutants were prepared by labeling the single cysteine with iodoacetamide. Donor-acceptor-labeled mutants were created by separate reactions with one, two, or three of the following reagents: (1) 5-iodoacetamidosalicylic acid, (2) 7-iodoacetamidocoumarin-4-carboxylic acid, and (3) 5-({2-[(iodoacetyl)amino]ethyl}amino)naphthalene-1-sulfonic acid (IAEDANS). Labeling conditions, removal of unlabeled protein, and chromatographic purification procedures have been described previously.[39] An example demonstrating sample purity can be found in Figure S5 of the Supporting Information.

Equilibrium Measurement. The protein sample concentration was determined according to the absorbance spectrum using the following molar extinction coefficients: ε_{278} = 16000 M^{-1} cm^{-1}, ε_{308} = 3200 M^{-1} cm^{-1}, ε_{340} = 16000 M^{-1} cm^{-1}, and ε_{336} = 5700 M^{-1} cm^{-1} for AK-DO_{IAA}, AK-DA_{Sal}, AK-DA_{Cca}, and AK-DA_{AEDANS}, respectively. Absorbance spectra were recorded using an AVIV model 17DS UV−vis−IR spectrophotometer (Aviv Biomedical, Lakewood, NJ).

Far-UV CD spectra were recorded using an AVIV model 62A DS CD spectropolarimeter (Aviv Biomedical). For each sample, five scans were determined, and the results were averaged. The protein sample concentration was 10 μM in 20 mM Tris-HCl (pH 7.8). CD measurements were taken using a 1 mm cuvette at 25 °C. The enzymatic activity was determined for all mutants as described by Ratner et al.[35] in the direction of ADP formation (MgATP + AMP ↔ MgADP + ADP) by a spectrophotometric assay based on a pyruvate kinase−lactate dehydrogenase coupling system.[40]

The time-correlated single-photon counting (TCSPC) method was used to measure the tryptophan fluorescence decay time (see Table S3 of the Supporting Information). The instrument, data collection, and analysis methodology have been described previously.[37] The protein sample concentration was 15 μM in 20 mM Tris-HCl (pH 7.8) at 25 °C.

Stopped-Flow Experiments Monitored by Total Fluorescence Acquisition. Kinetic measurements were performed using a stopped-flow SFM 400 instrument (Bio-Logic). Refolding experiments were conducted using two-step dilution (double jump) to minimize the effect of proline isomerization.[38] A protein sample (15 μM) under folding conditions [50 mM Tris-HCl (pH 8)] was first mixed (1:1) with 4 M Gnd-HCl dissolved in 50 mM Tris-HCl (pH 8). After a 3 s denaturation period, refolding was initiated with a second dilution (1:5.5) against 50 mM Tris-HCl (pH 8). Tryptophan excitation was set to the 297 nm line of a mercury arc lamp using a monochromator. A bandpass filter (Semrock 357/44) was used for measurements of tryptophan emission. Measure-

dx.doi.org/10.1021/bi500069w | *Biochemistry* 2014, 53, 3169−3178

Table 1. Labeling Plan and Structural Elements Studied as Part of the FRET Experiments

segment[a]	position[b]		acceptor dye[c]			nomenclature[d]	structure[e]
	D	A	Sal	Cca	AEDANS		
AK (1−6)	−2	8		√	√	AK-DA$_{Cca/EDANS}$ (−2, 8)	strand β_1
AK (79−85)	86	79	√	√	√	AK-DA$_{Sal/Cca/EDANS}$ (86, 79)	strand β_3
AK (104−110)	111	102		√	√	AK-DA$_{Cca/EDANS}$ (111, 102)	strand β_4
AK (1−26)	21	−2	√			AK-DA$_{Sal}$ (21, −2)	loop I
	24	−2	√	√	√	AK-DA$_{Sal/Cca/EDANS}$ (24, −2)	
	28	−2		√	√	AK-DA$_{Cca/EDANS}$ (28, −2)	
AK (1−86)	73	−2	√			AK-DA$_{Sal}$ (73, −2)	loop III
	75	−2	√		√	AK-DA$_{Sal/Cca}$ (75, −2)	
AK (1−111)	102	−2	√			AK-DA$_{Sal}$ (102, −2)	loop IV

[a]Chain segment that forms the subdomain structure to be studied, represented by its N and C boundaries. [b]Residues selected for mutation and labeling of each selected subdomain element. These are in most cases not at the exact structural ends of the element because of the labeling considerations, as described in the text. [c]In each mutant, the donor was a tryptophan residue and the engineered cysteine was labeled by an acceptor that is one of the three reagents listed here. Some mutants were labeled by more than one acceptor so the measurements could be repeated using pairs of different characteristics (R_o, size, hydrophobicity, etc.) for cross check and global analysis. [d]Representation of each doubly labeled mutant in the text. [e]Subdomain structural elements identified by each mutant.

ments were taken using the μFC-08 cell (Bio-Logic) with a dead time of 0.8 ms under the described experimental conditions. All of the solutions used for stopped-flow experiments were filtered through a 0.22 μm pore filter (Millipore) and measured at 25 °C.

Determination of ETE Values during Refolding. Kinetic measurements of each mutant were repeated at least six times, averaged, and corrected for background noise. Measurements on each set of mutants were repeated at least twice using different preparations. The change in energy transfer efficiency was determined using

$$E(t) = \frac{F_D(t) - F_{DA}(t)C_{eq}}{F_D(t)}$$

where $F_D(t)$ is the fluorescence intensity of the single tryptophan in a DO mutant and $F_{DA}(t)$ is the fluorescence intensity of the single tryptophan in a DA mutant. C_{eq} is a constant factor for correction of small deviations between the concentrations of the separately measured DO and DA traces. C_{eq} was derived from the trFRET experiments under folding conditions, which are equivalent to the end (plateau) of the kinetics experiment.

Stopped-Flow Double Kinetics Experiment. The system and data analysis used for the double kinetics experiments were recently described.[34,37]

RESULTS

Overall Strategy: FRET-Based Monitoring of the Pathways of Folding of Selected Subdomain Structural Elements, *in Situ*. The experimental design utilizes a FRET-based method for monitoring changes in intramolecular distances between specifically labeled residues that report the folding status of individual selected subdomain structural elements. Subdomain structures of interest, either the ends of native state closed long loops or the ends of segments that form native state β strands, were labeled by excitation donor and acceptor moieties. The first step was determination of the segmental end-to-end distance distribution in each mutant under folding and denaturing conditions at equilibrium. These distributions were used as a reference for the evaluation of the extent of folding of the labeled elements at each time point in the kinetics experiments. Refolding was initiated by dilution of a denaturant by the stopped-flow technique, and the time-dependent FRET efficiency was monitored both by intensity measurements (determination of the mean transfer efficiency, $\langle E \rangle$) and by trFRET using the double kinetics method, which yields the transient distance distributions.[37]

Labeling Plan: Selection of Subdomain Structural Elements To Be Monitored by FRET-Based Double Kinetics Experiments. Six pairs of sites at the ends of subdomain structures of interest were labeled in six sets of mutants (Table 1): (a) the N-terminal loop [residues 1−24 (Figure 1a and Figure S1 of the Supporting Information)], which is a typical elementary long closed loop structure; (b) two other loop elements [residues 1−86 and 1−109 (Figure 1b)], which represent "merged" loop elements, i.e., long segments (>40 residues) whose ends are in close contact, stabilized by hydrophobic interactions that also enclose at least one elementary loop within its boundaries (see Figure S1 of the Supporting Information); and (c) three of the five β strands that constitute the core (parallel) β sheet were labeled to study the rate of folding of secondary structure elements [β_1, residues 1−6; β_3, residues 79−85; and β_4, residues 104−110 (Figure 1a)].

The labeling strategy was based on incorporation of a single tryptophan (at residue n) and a single cysteine (residue m) at the ends of each element.[39,41,42] The cysteine (residue m) was then reacted with either 5-amidosalicylic acid (Sal), 7-acetamido-coumarin-4-carboxylic acid (Cou), or AEDANS [AK-DA$_{Sal}$ (n−m), AK-DA$_{Cca}$ (n−m), and AK-DA$_{AEDANS}$ (n−m), respectively] to create FRET pairs. A sample of each Trp-Cys mutant was reacted with iodoacetamide (IAA) and used as the "donor only" mutant [AK-D$_{ONLY}$ (n−m)]. The pairs had critical Förster distances (R_0) of 18, 22, and 24 Å for tryptophan−salicylic acid, −AEDANS, and −coumarin pairs, respectively. This allowed reliable determination of intarmolecular distances in the range between 9 and 36 Å. Replacement of any of the six N-terminal residues caused a loss of expression, which is an indication of their importance for the folding mechanism. To label the N-terminus of the AK molecule, we extended the polypeptide backbone using a four-residue insert (Met-Lys-Cys-Ala). The inserted Cys residue at position −2 was labeled in mutants designed to study the folding of the closed loop structures and the β_1 strand. Only surface-exposed residues were mutated to minimize the possible perturbation of

dx.doi.org/10.1021/bi500069w | Biochemistry 2014, 53, 3169−3178

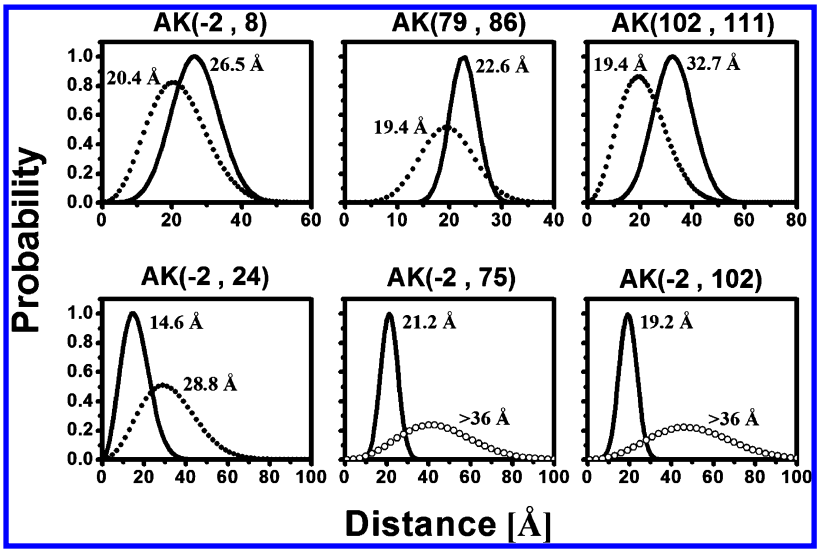

Figure 2. Segmental end-to-end distance distributions of the six labeled segments under folding and denaturing conditions (0.3 and 2 M Gnd-HCl, respectively). Folded (—) and denatured (●) state distributions are presented together with the mean of the segmental end-to-end distance distribution. Under folding conditions (0.3 M Gnd-HCl, 50 mM Tris-HCl, pH 7.8, and 25 °C), the mean distance between positions −2 and 8 (β_1), positions 79 and 86 (β_3), and positions 102 and 111 (β_4) was comparable (±2 Å) to the expected distance calculated from the crystal structure of apo-AK. For all the loop mutants [AK (−2, 24), AK (−2, 75), and AK (−2, 102)], the distance separation under denaturing conditions (2 M Gnd-HCl, 50 mM Tris-HCl, pH 7.8, and 25 °C) was higher than the folded state mean EED. The mean EED distributions obtained for the two long segments (residues −2 to 75 and −2 to 102) are only approximations because of the low transfer efficiency measured under denaturing conditions (○). The mean EED of the β strand structures was shortened under denaturing conditions compared to that of the folded state, reflecting the stretched conformation of the chain when it adopts a β strand structure. For all mutants, the FWHM values were highest in the denatured state, which indicates a heterogeneous ensemble of substates. Distance distributions were obtained from a global analysis of the donor fluorescence decay measured in the presence and absence of two different acceptors (see Table S3 of the Supporting Information). The protein concentration was 20 μM under both folding and denaturing buffer conditions.

Table 2. Parameters (mean and FWHM) of the Segmental End-to-End Distance Distributions Obtained for the Set of Doubly Labeled Mutants under Equilibrium Folding and Denaturing Conditions[a]

	0.3 M Gnd-HCl		2 M Gnd-HCl	
position[b]	r_{mean}[c] (Å)	FWHM[d] (Å)	r_{mean}[c] (Å)	FWHM[d] (Å)
AK (−2, 21)	24.6 (24.1−24.9)	15 (13−18)	out of range[e]	out of range[e]
AK (−2, 24)	14.6 (13.2−15.5)	14 (13−15)	28.8 (27.9−31.2)	30 (28−34)
AK (−2, 28)	23.4 (23.0−23.4)	6 (5−8)	29.6 (24.0−28.3)	28 (21−29)
AK (−2, 73)	23.3 (22.9−23.4)	11 (10−13)	out of range[e]	out of range[e]
AK (−2, 75)	21.2 (17.9−18.5)	7 (6−8)	out of range[e]	out of range[e]
AK (−2, 102)	19.2 (19.1−20.0)	8 (7−9)	out of range[e]	out of range[e]
AK (−2, 8)	27.0 (26.7−28.1)	9 (6−11)	19.6 (19.6−20.6)	20 (14−20)
AK (79, 86)	22.6 (22.3−22.9)	4 (3−5)	19.4 (18.3−20.1)	11 (8−14)
AK (102, 111)	32.7 (32.7−33.0)	16 (13−18)	19.4 (18.3−19.8)	20 (18−24)

[a]Comparison of the experimental mean intramolecular distances measured under folding conditions and those expected on the basis of the crystal structures shows reasonable agreement when the contribution of the linkers of the probes is taken into account. [b]Labeled mutants identified by the two mutated and labeled sites. [c]Mean of the segmental end-to-end distance distribution (95% confidence range given in parentheses). [d]FWHM of the segmental end-to-end distance distributions (95% confidence range given in parentheses). [e]Under denaturing conditions, the transfer efficiency between the labeled ends of the long segments was too low for statistical analysis.

the folding mechanism of the mutants. For selected elements, two or three sets of mutants were prepared. As an example, the folding of the N-terminal loop was monitored by mutants labeled at positions −2 and 21, position 24, or position 28. The combination of experiments in which structural elements were labeled by different FRET pairs (with different R_o values) and mutants in which such elements were labeled at different residues reduced the uncertainty in the combined results and provided internal controls.

Control Experiments. The extent of possible structural perturbation of the AK molecule due to the genetic and chemical modifications introduced in the labeling procedure was evaluated in a series of control experiments. Each mutant was tested by high-performance liquid chromatography analytical chromatography, absorption and emission spectra, CD spectroscopy, and an enzymatic activity assay. All tested mutants demonstrated similar (within error) far-UV CD spectra, which also closely overlapped with the wild type (wt) AK far-UV CD spectra (see Figure S2 of the Supporting Information). Enzymatic activity, which is highly sensitive to minor structural changes or electrostatic conditions near the active site, with one exception was kept in the range of 10−70% relative to the specific activity of wt AK (Table S1 of the Supporting Information). The reduction was more pronounced

dx.doi.org/10.1021/bi500069w | Biochemistry 2014, 53, 3169−3178

for mutants in which residues close to the active site were mutated. These control experiments confirmed that the labeled mutants retained the capacity for folding to the native structure and were suitable for this comparative folding study.

Distributions of the Intramolecular Distances in the Labeled Segments in the Fully Folded and Denatured States. Distance distributions were determined by analysis of trFRET measurements under both folding and unfolding conditions [in the presence of 0.3 and 2 M Gnd-HCl, respectively (see Figure 2)]. The results listed in Table 2 confirm the significant changes in the computed mean of each segmental end-to-end distance (EED) distribution, which allowed us to monitor their folding transition by the trFRET measurements. The values obtained under folding conditions were close to those expected distances estimated from the crystal structure of the substrate free molecule (PDB entry 4AKE), considering the dimensions of the probes. The labeled mutants were unfolded in 2 M Gnd-HCl solutions as shown by far-UV CD spectra,[38] the distributions of several intramolecular distances,[37,38,42] the uniformity of the fluorescence lifetime of tryptophan residues (Table S3 of the Supporting Information), and the observation that the mean values and the corresponding width of the distributions obtained for the shorter segments under unfolding conditions were comparable to the values expected for unstructured chains with similar lengths.[43]

Global versus Local Refolding Kinetics Monitored by Fluorescence Intensity Measurements: Kinetics of the Global Transition. Folding kinetic measurements were initiated using a two-step (double jump) stopped-flow mixing procedure (as described in Materials and Methods).[38] This setup was expected to allow pre-transition state events to be directly explored, on the basis of its experimental dead time (1 ms) and considering the global folding rate of AK (0.5 s^{-1}). The folding kinetics of AK mutants were examined at two levels of protein organization. Global folding kinetics were monitored by 1-anilinonaphthalene-8-sulfonic acid (ANS) emission intensity,[44] capturing the transition from a partially organized intermediate (which binds ANS) to the well-packed native state (which does not bind ANS). For all tested mutants, the folding rate (determined by the emission intensity of ANS) ranged between 0.1 and 0.6 s^{-1} (see Table S2 of the Supporting Information), which is similar to the folding rate of wt AK (0.5 s^{-1}). A second reference measurement was obtained by recording the changes in the tryptophan emission intensity and fluorescence lifetime in the nine labeled sites in the absence of an acceptor (see Table S2 of the Supporting Information). An immediate increase was expected because of the decrease in the denaturant concentration. This was followed by a slow change (an increase or decrease depending on each local structure) at a rate similar to (or lower than) that of the change in the ANS emission intensity.

The tryptophan residues are located at nine different sites and thus reflect a global change, yet both the tryptophan and ANS emissions are sensitive to local conformational changes. Therefore, it is no surprise that in a few cases, the traces of the change in the fluorescence intensity either of the ANS or of the tryptophan emission were fit with two rate constants reflecting local effects. In most of these cases, the second rate constant was in the same time regime as the first rate constant. Evidence of a complex folding transition of loop I was obtained by the double kinetics experiment (see below). Despite the variations described above, the common component of the folding rate found for all mutants by the kinetics of the change in the ANS and tryptophan emission suggests that the labeling modifications did not alter the global folding kinetics.

Kinetics of Subdomain Transitions. On the background of the rate of the global transition, the rates of each labeled subdomain element were obtained by determination of the mean FRET efficiency change during the global folding transition (Figure 3A and Figure S3 of the Supporting Information). Three kinetic patterns of subdomain folding were observed (Figure 3B).

Pattern I. No fast initial change in FRET efficiency was seen along with a transition to the native state level at a rate similar to that of the global folding transition. Such a pattern implies that this segment is still unordered in the collapsed state and folds to nativelike structure only during the global folding transition. That was the case for labeled mutants AK (−2, 8) and AK (79, 86), which monitor the folding status of strands β_1 and β_3, respectively.

Pattern II. Full recovery of the native transfer efficiency occurred within the 1 ms dead time of the mixing device. Such results imply that nativelike contacts were assembled during the early phase of the folding transition. That was the case for mutants AK (−2, 24) and AK (−2, 75), which probed the closure of loop I and merged loop III, respectively, occurring within the dead time of the instrument.

Pattern III. In terms of biphasic kinetics, the partial burst phase change was followed by a slow refolding phase. This implies partial early folding of these elements and continuation only at the rate of the global folding transition. This was the case for mutants AK (−2, 102) (merged loop IV) and AK (102, 111) (strand β_4).

These kinetic results (see Table S2 of the Supporting Information) reveal hidden features of the hierarchic folding transition of the CORE domain of this large molecule. The two mutants that monitored the immediate closure of loops I and IV (pattern II) report nativelike proximity of the ends of each one of these two loops, at a rate 3 orders of magnitude faster than the global folding rate. At the time of initial loop closure, the segments that form the native β_1 and β_3 strand structure are disordered. More details demonstrating the selectivity of structure formation were revealed by the double kinetics experiments.

Double Kinetics Experiment: Development of the Distributions of Intramolecular Distances in the Selected Subdomain Elements. Determination of mean intramolecular distances based on mean energy transfer efficiency (obtained by emission intensity measurements) can be misleading when ensembles of multiple conformers are studied.[28] The mean of a distribution of intramolecular distances determined by analysis of trFRET measurements is a more reliable representation of the mean intramolecular distances in the molecule being studied. The width of the distribution gives additional information about the degree of order of the labeled chain segments.[28,45] In the double kinetics experiment, fast recording of a series of fluorescence decay curves during the folding transition yields time series of transient distributions of selected (based on the position of the double labeling) intramolecular distances. The result is a detailed record of the degree of order of every labeled chain segment along the pathway of folding at millisecond time resolution for the chemical transition, and picosecond resolution at the spectroscopic level (e.g., fluorescence lifetime). Equipped with the ability to quickly acquire

dx.doi.org/10.1021/bi500069w | *Biochemistry* 2014, 53, 3169−3178

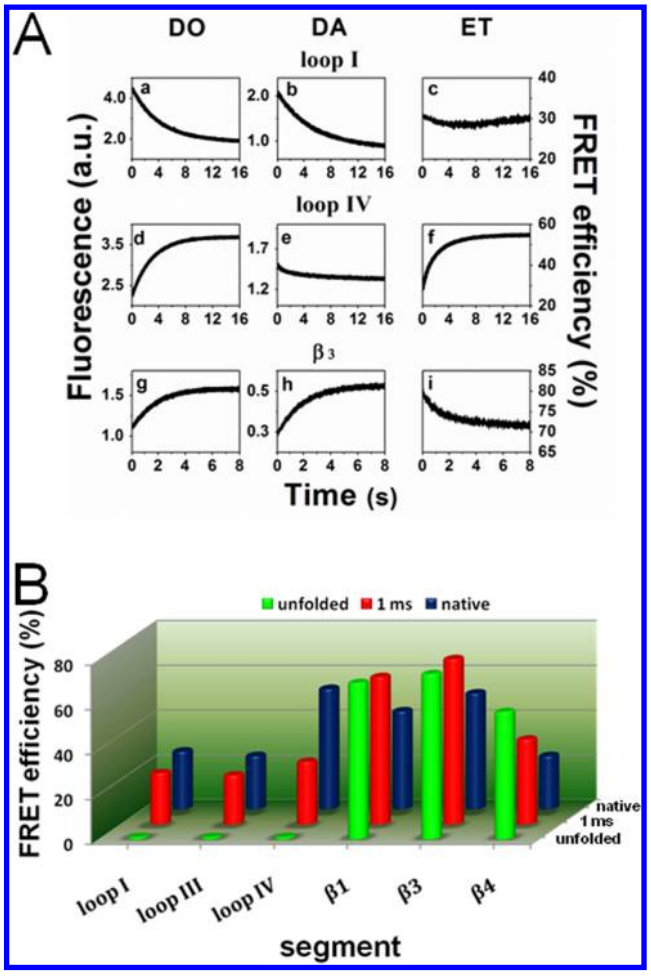

Figure 3. Refolding kinetics monitored by the change in mean transfer efficiency. (A) Each row of panels represents results obtained for one labeled mutant [AK (−2, 24), AK (−2, 102), and AK (79, 86) from top to bottom, respectively]. Each column of panels represents a different class of experiment. (1) The left column demonstrates the change in donor fluorescence in the absence of an acceptor (donor only labeled mutants). (2) The middle column illustrates the change in the donor fluorescence in the presence of an acceptor (donor- and acceptor-labeled mutants). (3) The right column corresponds to the evaluated change in FRET efficiency during the refolding transition (for the complete data set, see Figure S3 of the Supporting Information). (B) FRET efficiencies of six labeled mutants obtained under unfolding conditions (green), 1 ms after the change to folding conditions (red), and under folding conditions (blue). Nativelike FRET efficiencies were fully restored 1 ms after refolding had been initiated at the N-terminal loop segment (loop I) and the merged loop segment (loop III, between β_1 and β_3). These loops are closed within the mixing dead time. The FRET efficiency between the ends of strands β_1 and β_3 was comparable to the values obtained for the unfolded state at the end of the dead time of the kinetic experiment. These segments appear to remain disordered during the initial phase of the transition. Thus, nonlocal contacts are formed long before the formation of the β strands in the CORE domain of the AK molecules.

tryptophan fluorescence decay curves during the refolding transition, we performed refolding experiments in a double kinetics mode using two of the labeled mutants: AK (−2, 24), which monitors the N-terminal loop I, and AK (79, 86), which monitors changes in the conformation of strand β_3. Tryptophan decay curves were recorded 15 ms, 1.5 s, 3 s, 4.5 s, and 5 min after mixing (Figure 4A).

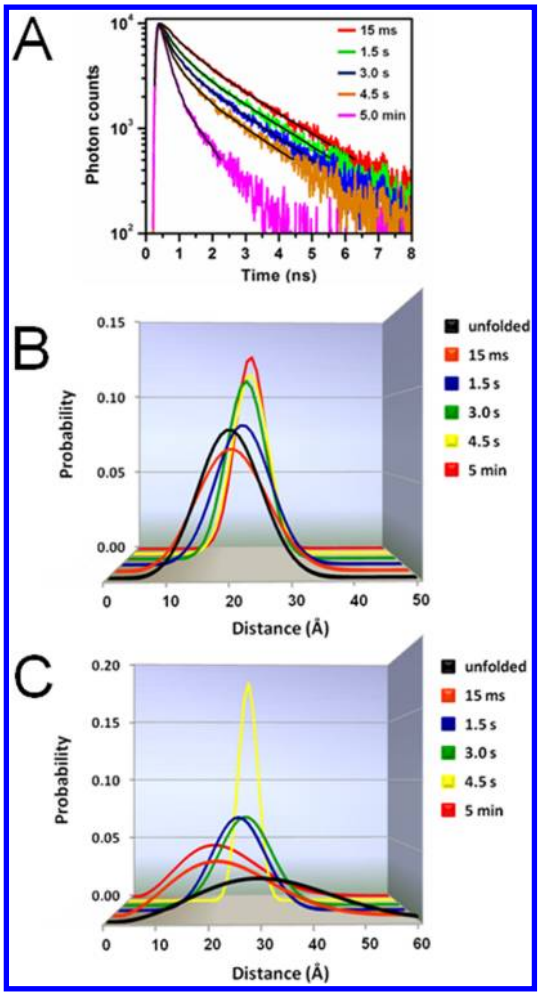

Figure 4. Series of transient segmental end-to-end distance distributions monitoring the progress of folding of the N-terminal loop I and strand β_3 obtained by trFRET measurement in the double kinetics experiment. (A) Series of fluorescence decay curves of tryptophan 24 in the absence of an acceptor at position −2. Each curve was collected during the 2 ms time interval at the predetermined refolding time point as indicated by the color code. The black traces represent the best fit calculated decay curves. The gradual reduction of the characteristic of the probe (mean fluorescence lifetime) that reflects local structural changes is in contrast to the immediate change in the distance between the ends of loop I (loop closure), which was found by global analysis of the series of DO and DA experiments. (B) Series of transient distributions of the distances between the ends of the segment forming strand β_3 obtained by global analysis of the DO and DA double kinetics experiment of mutant AK (79, 86). The distance distribution of the 15 ms species (orange) fully overlaps with that obtained at equilibrium under unfolding conditions (black). The narrow nativelike EED distribution characteristic of the extended conformation of the native strand structure is complete only 3 s after the initiation of refolding (green). (C) Series of transient distributions of the distances between the labeled ends of the N-terminal loop I obtained by global analysis of transient fluorescence decay curves of the Trp residue in the DO and DA mutants by means of the double kinetics experiment. The 15 ms distribution (orange) fully overlaps with the native fold distribution (red). Thus, this loop is closed within or immediately after the initiation of folding. The shift in the mean of the distribution to a longer distance and the reduction of the corresponding width values at intermediate time points (blue, green, and yellow) indicate that early formed closed loop structure is later deformed during the slow ordering of the chain segments that seem to perturb the loop closure interaction.

dx.doi.org/10.1021/bi500069w | *Biochemistry* 2014, 53, 3169−3178

Table 3. Time Dependence of the Distributions of the Segmental End-to-End Distances during the Full Duration of the Folding Transition[a]

	AK (−2, 24)[e]		AK (79, 86)	
refolding time[b]	r_{mean}[c] (Å)	FWHM[d] (Å)	r_{mean}[c] (Å)	FWHM[d] (Å)
unfolded	28.8 (27.9−31.2)	30 (28−34)	19.4 (18.3−20.1)	11 (8−14)
15 ms	20.7 (17.1−23.6)	22 (14−25)	19.5 (16.5−20.1)	12 (3−18)
1.5 s	24.9 (23.0−24.8)	11 (3−23)	21.4 (20.8−21.6)	10 (6−13)
3.0 s	26.3 (25.4−27.3)	12 (6−16)	21.9 (21.3−22.2)	6 (3−7)
4.5 s	26.8 (25.8−30.7)	4 (4−29)	22.7 (22.5−22.8)	6 (5−12)
native	18.8 (17.4−21.0)	19 (11−26)	22.7 (22.5−22.9)	5 (3−7)

[a]The mean of the EED distribution obtained for the segment that forms strand β_3 in the native state is gradually increased during the first 1.5 s of the folding pathway, and mainly after that time point, the width of the distribution is reduced to the native value. These two parameters reflect two characteristics of subdomain folding: the over dimensions of the segment and its degree of order. [b]Time that passed since the end of the initiation of folding by the change in solvent from denaturing (2 M Gnd-HCl) to folding (0.3 M Gnd-HCl) conditions. [c]Mean of the segmental end-to-end distance (95% confidence range given in parentheses). [d]Full width at half-maximum of the segmental end-to-end distance distribution. [e]Interestingly, the data obtained for this mutant labeled at loop I show a fast decrease in the distance between the labeled sites, which is then increased again and only at the latest phase of the folding pathway returns to the loop closure.

Each set of measurements included determination of the fluorescence decay of the tryptophan residues in the absence and presence of an acceptor. Thus, for each mutant, three decay curves were generated for each time window (donor only, donor in the presence of acceptor A, and donor with acceptor B). Finally, all three decay curves were globally analyzed to construct transient distance distributions throughout the refolding transition (Figure 4B,C and Table 3). The distance distributions obtained for the 15 ms intermediate state corroborate the conclusions obtained from analyses of kinetics of the emission intensity measurements. The earliest measured distribution of the distance between the ends of the segment that forms strand β_3 (the distance between residues 79 and 86) was the same as that obtained in the denatured state (Figure 4B and Table 3). During the first 1.5 s of refolding, the mean of that distribution increased and approached the native distribution, with a full overlap attained from 3 s (and onward). The full width at half-maximum (FWHM) of the distribution was gradually reduced at the rate of the global folding transition of the AK molecule. Apparently, the stretched conformation of strand β_3 is stabilized between 15 and 1500 ms after the initiation of folding (a time frame that is still prior to the rate-limiting folding step).

In sharp contrast to the gradual transition to the native end-to-end distance distribution of strand β_3, shortly after the initiation of the folding pathway (15 ms), the mean of the distribution between the labeled ends of the N-terminal loop [loop I, measured in mutant AK (−2, 24)] is approximately the same as that of the final folded state [approximately 8 ± 3 Å shorter than that of the denatured ensemble (see Figure 4C and Table 3)]. Thus, the double kinetics experiment confirms the conclusion that the loop ends attain a closed nativelike contact in the collapsed state, long before the transition of the secondary structure element β_3 to its native full length.

However, the time series of distance distributions obtained by the double kinetics experiment reveals additional interesting features of the folding pathway of the CORE domain of AK. At 1.5 s, the mean of the distribution increased while its FWHM decreased; at 4.5 s, the FWHM of the distribution was further reduced as if the extent of conformational variation was much reduced. Finally, when the global native fold of the whole molecule was established at equilibrium, the distribution returned to the mean and FWHM observed at the earliest measurement (Figure 4C and Table 3). Interestingly, the perturbation of the closed loop structure seems to be coincident with the secondary structure formation of strands β_3 and β_1. These findings show that although the loop is first closed in the collapsed state, when the β_1 strand included in this loop is still relaxed and the rest of the chain is disordered, the "slow" folding of the other elements of the CORE domain affects the closed loop state. The double kinetics experiments reveal fine details of the dependence of the subdomain conformation on transitions of other structural elements of the AK molecule. Thus, the folding of the subdomain element is context-dependent.

DISCUSSION

The experiments described here were designed to test the hypothesis that the long loop closure transition is an essential element of the initiation of the folding transition, which directs the protein refolding pathway.[27,28] We demonstrate the power of monitoring the progression of folding of individual subdomain elements within the intact molecule, *in situ*. This is particularly significant because every interaction in a protein molecule is influenced by its neighboring structural elements, which are rapidly altered as the folding proceeds. The elementary steps of the transition are stochastic, and therefore, the initial structures of the folding pathway are very diverse and can be described only in statistical terms. Methods that detect localized structural changes such as fluorescence parameters of natural or chemically attached probes, circular dichroism spectroscopy, or small-angle X-ray scattering cannot detect specific loop closure events in the diverse ensemble of refolding protein molecules. We therefore utilized the double kinetic methods to capture transient intramolecular distance distributions of preselected subdomain elements.

The rate of refolding of the AK molecule is in the range of 0.5 ± 0.3 s^{-1}. We monitored the kinetics of the folding transition of six subdomain elements in the CORE domain of the molecule and found differences of 3 orders of magnitude in their folding rates.

Previously, we demonstrated that the loop formed by the AMP_{bind} domain (loop II) is closed within the dead time of the stopped-flow mixing device.[37,38] That loop forms a separate domain that might be fast folding. In this study, we found that the N-terminal loop (loop I), which is a typical subdomain structure, is closed at the initiation of folding. We further found that additional loop structure that is part of the CORE domain

dx.doi.org/10.1021/bi500069w | *Biochemistry* 2014, 53, 3169−3178

is also closed within the first millisecond of folding. This is the longer, "merged" loop (loop III), which is formed by the 77 N-terminal residues of the AK molecule. It includes the two smaller N-terminal loops (I and II). In fact, the further extended merged loop (loop IV), from the N-terminus to strand β_4, labeled by residues −2 and 102, is only partially closed soon after the initiation of folding.

In sharp contrast, the expansion of the segments forming strands β_1, β_3, and β_4 to native end-to-end distance occurs at a much later phase of the folding transition. We previously showed that strand β_9 (the fifth strand in the suprasecondary structure of the CORE domain of AK) and helix α_8 are also disordered prior to the global folding transition.[35] Slow formation of secondary structures was also recently reported by Englander et al.,[46,47] who used hydrogen exchange detected by nuclear magnetic resonance and mass spectrometry. Another loop that was tested, the LID domain loop (residues 121−155), did not show this very early closure transition (see Figure S4 of the Supporting Information). The very early long loop closure event of the N-terminal loop I may be driven by very effective specific NLIs between clusters of residues at the ends of this loop. The very fast closure of the distance between residues −2 and 75 (loop IV), which are widely separated along the chain, may be the result of contributions of several factors: (a) the effectiveness of nonlocal interactions between clusters of residues in the segments that form β_1 and β_3 native strands independent of the formation of the strand's native structure, (b) closure of the long loops included in the 77-residue segment (N-terminal loop I and AMP_{bind} loop II),[38] and (c) additional interactions in the folding core of the CORE domain.

The current FRET experiments monitored the distribution of distances between the ends of loops I−IV. An alternative interpretation of the fast closure of the distances between the ends of the loops might be fast nonspecific compaction of the whole chain segment that connects the two labeled residues. Such interpretation is very unlikely for several reasons. (a) Many experiments show that the dimensions of ensembles of nonspecifically collapsed protein molecules are significantly larger than those of the compact native state.[48−50] Most of the chain segments are highly solvated and swollen. (b) At least for loops I and II, the loop's end-to-end distance distributions were nativelike at the moment of the end of the mixing dead time. That is in sharp contrast to the non-nativelike intramolecular distances of other segments, emission intensities, and lifetimes of Trp residues and of ANS, which became nativelike during the slow refolding kinetics. (c) The distance between residues 58 and 86, which is internal in loops II and III and hence is expected to be affected by nonspecific condensation of the loops' segment, was not nativelike at the end of the mixing dead time.[51] A slow change toward the native distance was observed in contrast to the fast formation of the nativelike distance of the loops' ends. Indeed, an open question is whether the loop closure is supported by formation of secondary structure elements formed in the native state by the loops' segments. So far, we have found evidence of slow formation of a few β strands, and the role of helices will be further studied

The time series of the transient distributions of N-terminal segmental end-to-end distances of loop I underscore the importance of studying the kinetics of folding of structural elements *in situ,* and the strength of the FRET-detected double kinetics method. The observation that the rapidly closed native loop is reopened and subsequently reclosed as part of the folding pathway of the protein molecule is intriguing. One possible interpretation is that the closed loop has an essential role in the initial phase of folding but is then relaxed as a result of subsequent folding steps or to allow the folding of additional elements. This observation highlights the complexity of the hierarchic folding transition and the context dependence of the folding of the subdomain elements. Transient non-native contacts were previously reported in folding pathways of some globular proteins.[52] These might be viewed as temporary scaffolds that are formed and then removed. The well-established "contact order correlation"[53] seems to be at odds with the loop hypothesis. However, the contact order correlation is summed over the entire polypeptide chain and hence is not sensitive to a small number of closed loops that might affect the folding rate. Furthermore, that correlation refers to the rate of global folding (the formation of the TSE), while the loop hypothesis describes the initiation of folding, which in the present case is 3 orders of magnitude faster.

The results presented here support the sequential collapse model for protein folding presented by Bergasa-Caceres and Rabitz.[54] The "closed loop hypothesis" can be viewed as an extension of the nucleation condensation mechanism. The key feature of the nucleation condensation mechanism is the formation of "contact-assisted" secondary structure elements that form the folding nucleus in the TSE.[55] Thus, the formation of secondary structures is coupled to formation of "long range contacts" that are stabilized by NLIs. The loop hypothesis assumes fast formation of nonlocal contacts independent of the formation of secondary structures at the initiation of folding. In this study, we find that three CORE domain β strands are formed only at the rate of the formation of the TSE and their change to native mean end-to-end distance is not coupled to the nonlocal contact formation. The node of the N-terminal loop (loop I) includes at least one side that has an unfolded secondary structure (β_1) in the first milliseconds of the folding pathway. Moreover, the node closing the long merged loop (loop III, which includes loops I and II) monitored by the probes attached to residues −2 and 75 seems to lie between two disordered segments that form β_1 and β_3, which are not stretched at the time of loop closure. These findings indicate that the interactions responsible for closure of these loops are not dependent on the secondary structure of the clusters forming the loop nodes.

The FRET methods probe specific structural changes. This is essential for creating a full description of the hierarchic sequence of the transitions that lead to the ensemble of transition state structures. Nonlocal contacts were detected by other methods (e.g., hydrogen exchange[46,47]), but FRET measurements are unique in their ability to directly yield intramolecular distances. This series of experiments emphasizes the fact that the closed long loop structures are part of the initial subdomain structures that are ordered at the initiation of the folding pathway, while the formation of the TSE and the folding of other sections of the chain occur at rates 3 orders of magnitude slower (Figure 3). The rapidly closed loops are associated with the N-terminal section of the CORE domain, and it is therefore reasonable to assume that they contribute to the formation of the folding nucleus. It is also reasonable to assume that the small number of rapidly closed loop structures can reduce the probability of proteolysis[56] or aggregation of the disordered molecules during their fluctuations leading to the transition state.

This study describes several novel findings that shed light on the earliest stages of protein folding. We demonstrate the

context dependence of folding of selected subdomains; the fast closure of two loops in the CORE domain of the AK molecule at the initiation of the folding pathway; the slow formation of three CORE domain β strands, even though those chain segments interact to close loops at a much earlier time in the folding pathway; the fast closure of the merged loop (III); and the transient reopening of the N-terminal loop (I) during the folding pathway. Together, these results provide strong support for the loop hypothesis.

■ ASSOCIATED CONTENT

Supporting Information

Figures that present a schematic representation of loop structures in the CORE domain of the AK molecule, the far-UV CD spectra, traces of the kinetics of changes in the emission intensity of the mutants, results of measurements of a slow loop, and the details of the preparative procedures and purity of the samples, a table of all rate constants obtained with different probes during the refolding transition of the mutants under study, and a table of mean fluorescence lifetimes of the Trp residues in the mutants. This material is available free of charge via the Internet at http://pubs.acs.org.

■ AUTHOR INFORMATION

Corresponding Author

*The Goodman Faculty of Life Sciences, Bar Ilan University, Ramat Gan, Israel 52900. E-mail: elisha.haas@biu.ac.il. Telephone: ++972-3-5318210 or ++972-54-627-0012. Fax: ++972-3-7369928.

Funding

This study was supported by grants from the Israel Science Foundation (ISF1464/10), the ISF-ICORE grant (1902/12), and the United States-Israel Binational Science Foundation (Grant 2011143).

Notes

The authors declare no competing financial interest.

■ ACKNOWLEDGMENTS

We are grateful to Mr. E. Zimerman, M. Schneeberg, and D. Freedman for excellent technical assistance. We are grateful to Gershon Hazan, Eitan Lerner, Gil Rahamim, and Asaf Grupi for their contributions and discussions.

■ ABBREVIATIONS

AA, acetamide; AK, *E. coli* adenylate kinase; DA, time-resolved measurement of donor emission in an AK molecule labeled with a donor and an acceptor; DA_{Sal} ($n-m$) or DAAED ($n-m$), AK mutant labeled with a donor (Trp residue) at residue n and an acceptor (aminosalicylic acid or AEDANS) at residue m; DO ($n-m$), AK mutant labeled with a donor (Trp residue) at residue n and a cysteine residue at residue m blocked by acetamide; EED, end-to-end distance; FRET, Förster type resonance excitation energy transfer; Gnd-HCl, guanidinium hydrochloride; IAA, iodoacetamide; Cou, acetamidocoumarin-4-carboxylic acid; LI, local interaction; NLI, nonlocal interaction; TCEP, tris(2-carboxyethyl)phosphine; TSE, transition state ensemble; trFRET, time-resolved FRET; FWHM, full width at half-maximum; PDB, Protein Data Bank.

■ REFERENCES

(1) Baldwin, R. L., and Rose, G. D. (1999) Is protein folding hierarchic? II. Folding intermediates and transition states. *Trends Biochem. Sci. 24*, 77−83.

(2) Englander, S. W., Mayne, L., and Krishna, M. M. (2007) Protein folding and misfolding: Mechanism and principles. *Q. Rev. Biophys. 40*, 287−326.

(3) Magg, C., Kubelka, J., Holtermann, G., Haas, E., and Schmid, F. X. (2006) Specificity of the initial collapse in the folding of the cold shock protein. *J. Mol. Biol. 360*, 1067−1080.

(4) Fersht, A. R. (1997) Nucleation mechanisms in protein folding. *Curr. Opin. Struct. Biol. 7*, 3−9.

(5) Chan, H. S., and Dill, K. A. (1991) Polymer principles in protein structure and stability. *Annu. Rev. Biophys. Biophys. Chem. 20*, 447−490.

(6) Kathuria, S. V., Guo, L., Graceffa, R., Barrea, R., Nobrega, R. P., Matthews, C. R., Irving, T. C., and Bilsel, O. (2011) Minireview: Structural insights into early folding events using continuous-flow time-resolved small-angle X-ray scattering. *Biopolymers 95*, 550−558.

(7) Roder, H., Maki, K., and Cheng, H. (2006) Early events in protein folding explored by rapid mixing methods. *Chem. Rev. 106*, 1836−1861.

(8) Ferguson, N., and Fersht, A. R. (2003) Early events in protein folding. *Curr. Opin. Struct. Biol. 13*, 75−81.

(9) Vendruscolo, M., Paci, E., Dobson, C. M., and Karplus, M. (2001) Three key residues form a critical contact network in a protein folding transition state. *Nature 409*, 641−645.

(10) Fersht, A. R. (2000) Transition-state structure as a unifying basis in protein-folding mechanisms: Contact order, chain topology, stability, and the extended nucleus mechanism. *Proc. Natl. Acad. Sci. U.S.A. 97*, 1525−1529.

(11) Lindorff-Larsen, K., Vendruscolo, M., Paci, E., and Dobson, C. M. (2004) Transition states for protein folding have native topologies despite high structural variability. *Nat. Struct. Mol. Biol. 11*, 443−449.

(12) Kim, P. S., and Baldwin, R. L. (1982) Specific intermediates in the folding reactions of small proteins and the mechanism of protein folding. *Annu. Rev. Biochem. 51*, 459−489.

(13) Ionescu, R. M., and Matthews, C. R. (1999) Folding under the influence. *Nat. Struct. Biol. 6*, 304−307.

(14) Go, N., and Taketomi, H. (1978) Respective roles of short- and long-range interactions in protein folding. *Proc. Natl. Acad. Sci. U.S.A. 75*, 559−563.

(15) Taketomi, H., Ueda, Y., and Go, N. (1975) Studies on protein folding, unfolding and fluctuations by computer simulation. I. The effect of specific amino acid sequence represented by specific inter-unit interactions. *Int. J. Pept. Protein Res. 7*, 445−459.

(16) Goldstein, R. A., Luthey-Schulten, Z. A., and Wolynes, P. G. (1992) Optimal protein-folding codes from spin-glass theory. *Proc. Natl. Acad. Sci. U.S.A. 89*, 4918−4922.

(17) Govindarajan, S., and Goldstein, R. A. (1995) Optimal local propensities for model proteins. *Proteins 22*, 413−418.

(18) Abkevich, V. I., Gutin, A. M., and Shakhnovich, E. I. (1995) Impact of local and non-local interactions on thermodynamics and kinetics of protein folding. *J. Mol. Biol. 252*, 460−471.

(19) Anfinsen, C. B., and Scheraga, H. A. (1975) Experimental and theoretical aspects of protein folding. *Adv. Protein Chem. 29*, 205−300.

(20) Harrison, S. C., and Durbin, R. (1985) Is there a single pathway for the folding of a polypeptide chain? *Proc. Natl. Acad. Sci. U.S.A. 82*, 4028−4030.

(21) Rooman, M. J., Kocher, J. P., and Wodak, S. J. (1992) Extracting information on folding from the amino acid sequence: Accurate predictions for protein regions with preferred conformation in the absence of tertiary interactions. *Biochemistry 31*, 10226−10238.

(22) Wright, P. E., Dyson, H. J., and Lerner, R. A. (1988) Conformation of peptide fragments of proteins in aqueous solution: Implications for initiation of protein folding. *Biochemistry 27*, 7167−7175.

(23) Dill, K. A., Fiebig, K. M., and Chan, H. S. (1993) Cooperativity in protein-folding kinetics. *Proc. Natl. Acad. Sci. U.S.A. 90*, 1942−1946.

(24) Weikl, T. R., and Dill, K. A. (2003) Folding rates and low-entropy-loss routes of two-state proteins. *J. Mol. Biol. 329*, 585−598.
(25) Ristow, S. S., and Wetlaufer, D. B. (1973) Evidence for nucleation in the folding of reduced hen egg lysozyme. *Biochem. Biophys. Res. Commun. 50*, 544−550.
(26) Kihara, D. (2005) The effect of long-range interactions on the secondary structure formation of proteins. *Protein Sci. 14*, 1955−1963.
(27) Ittah, V., and Haas, E. (1995) Nonlocal Interactions Stabilize Long-Range Loops in the Initial Folding Intermediates of Reduced Bovine Pancreatic Trypsin-Inhibitor. *Biochemistry 34*, 4493−4506.
(28) Haas, E. (2005) The study of protein folding and dynamics by determination of intramolecular distance distributions and their fluctuations using ensemble and single-molecule FRET measurements. *ChemPhysChem 6*, 858−870.
(29) Leszczynski, J. F., and Rose, G. D. (1986) Loops in globular proteins: A novel category of secondary structure. *Science 234*, 849−855.
(30) Orevi, T., Rahamim, G., Hazan, G., Amir, D., and Haas, E. (2013) The loop hypothesis: Contribution of early formed specific non-local interactions to the determination of protein folding pathways. *Biophys. Rev. 5*, 85−98.
(31) Beals, J. M., Haas, E., Krausz, S., and Scheraga, H. A. (1991) Conformational studies of a peptide corresponding to a region of the C-terminus of ribonuclease A: Implications as a potential chain-folding initiation site. *Biochemistry 30*, 7680−7692.
(32) Beechem, J. M., Sherman, M. A., and Mas, M. T. (1995) Sequential domain unfolding in phosphoglycerate kinase: Fluorescence intensity and anisotropy stopped-flow kinetics of several tryptophan mutants. *Biochemistry 34*, 13943−13948.
(33) Ratner, V., and Haas, E. (1998) An instrument for time resolved monitoring of fast chemical transitions: Application to the kinetics of refolding of a globular protein. *Rev. Sci. Instrum. 69*, 2147−2154.
(34) Ben Ishay, E., Hazan, G., Rahamim, G., Amir, D., and Haas, E. (2012) An instrument for fast acquisition of fluorescence decay curves at picosecond resolution designed for "double kinetics" experiments: Application to FRET study of protein folding. *Rev. Sci. Instrum. 83*, 084301.
(35) Ratner, V., Amir, D., Kahana, E., and Haas, E. (2005) Fast collapse but slow formation of secondary structure elements in the refolding transition of *E. coli* adenylate kinase. *J. Mol. Biol. 352*, 683−699.
(36) Ratner, V., Sinev, M., and Haas, E. (2000) Determination of intramolecular distance distribution during protein folding on the millisecond timescale. *J. Mol. Biol. 299*, 1363−1371.
(37) Ben Ishay, E., Rahamim, G., Orevi, T., Hazan, G., Amir, D., and Haas, E. (2012) Fast subdomain folding prior to the global refolding transition of *E. coli* adenylate kinase: A double kinetics study. *J. Mol. Biol. 423*, 613−623.
(38) Orevi, T., Ben Ishay, E., Pirchi, M., Jacob, M. H., Amir, D., and Haas, E. (2009) Early closure of a long loop in the refolding of adenylate kinase: A possible key role of non-local interactions in the initial folding steps. *J. Mol. Biol. 385*, 1230−1242.
(39) Sinev, M., Landsmann, P., Sineva, E., Ittah, V., and Haas, E. (2000) Design consideration and probes for fluorescence resonance energy transfer studies. *Bioconjugate Chem. 11*, 352−362.
(40) Rhoads, D. G., and Lowenstein, J. M. (1968) Initial velocity and equilibrium kinetics of myokinase. *J. Biol. Chem. 243*, 3963−3972.
(41) Ratner, V., Kahana, E., Eichler, M., and Haas, E. (2002) A general strategy for site-specific double labeling of globular proteins for kinetic FRET studies. *Bioconjugate Chem. 13*, 1163−1170.
(42) Jacob, M. H., Amir, D., Ratner, V., Gussakowsky, E., and Haas, E. (2005) Predicting reactivities of protein surface cysteines as part of a strategy for selective multiple labeling. *Biochemistry 44*, 13664−13672.
(43) Grupi, A., and Haas, E. (2011) Segmental Conformational Disorder and Dynamics in the Intrinsically Disordered Protein α-Synuclein and Its Chain Length Dependence. *J. Mol. Biol. 405*, 1267−1283.
(44) Semisotnov, G. V., Rodionova, N. A., Razgulyaev, O. I., Uversky, V. N., Gripas, A. F., and Gilmanshin, R. I. (1991) Study of the "molten globule" intermediate state in protein folding by a hydrophobic fluorescent probe. *Biopolymers 31*, 119−128.
(45) Haas, E. (1989) Folding and dynamics of globular proteins studied by time resolved fluorescence spectroscopy. *Prog. Clin. Biol. Res. 289*, 157−170.
(46) Hu, W., Walters, B. T., Kan, Z. Y., Mayne, L., Rosen, L. E., Marqusee, S., and Englander, S. W. (2013) Stepwise protein folding at near amino acid resolution by hydrogen exchange and mass spectrometry. *Proc. Natl. Acad. Sci. U.S.A. 110*, 7684−7689.
(47) Englander, S. W., and Mayne, L. (1992) Protein folding studied using hydrogen-exchange labeling and two-dimensional NMR. *Annu. Rev. Biophys. Biomol. Struct. 21*, 243−265.
(48) Wu, Y., Kondrashkina, E., Kayatekin, C., Matthews, C. R., and Bilsel, O. (2008) Microsecond acquisition of heterogeneous structure in the folding of a TIM barrel protein. *Proc. Natl. Acad. Sci. U.S.A. 105*, 13367−13372.
(49) Yoo, T. Y., Meisburger, S. P., Hinshaw, J., Pollack, L., Haran, G., Sosnick, T. R., and Plaxco, K. (2012) Small-angle X-ray scattering and single-molecule FRET spectroscopy produce highly divergent views of the low-denaturant unfolded state. *J. Mol. Biol. 418*, 226−236.
(50) Haran, G. (2012) How, when and why proteins collapse: The relation to folding. *Curr. Opin. Struct. Biol. 22*, 14−20.
(51) Orevi, T., Ben Ishay, E., Pirchi, M., Jacob, M. H., Amir, D., and Haas, E. (2009) Early closure of a long loop in the refolding of adenylate kinase: A possible key role of non-local interactions in the initial folding steps. *J. Mol. Biol. 385*, 1230−1242.
(52) Voelz, V. A., Jager, M., Yao, S., Chen, Y., Zhu, L., Waldauer, S. A., Bowman, G. R., Friedrichs, M., Bakajin, O., Lapidus, L. J., Weiss, S., and Pande, V. S. (2012) Slow unfolded-state structuring in Acyl-CoA binding protein folding revealed by simulation and experiment. *J. Am. Chem. Soc. 134*, 12565−12577.
(53) Plaxco, K. W., Simons, K. T., and Baker, D. (1998) Contact order, transition state placement and the refolding rates of single domain proteins. *J. Mol. Biol. 277*, 985−994.
(54) Bergasa-Caceres, F., Ronneberg, T. A., and Rabitz, H. (1999) Sequential Collapse Model for Protein Folding Pathways. *J. Phys. Chem. B 103*, 9749−9758.
(55) Daggett, V., and Fersht, A. R. (2003) Is there a unifying mechanism for protein folding? *Trends Biochem. Sci. 28*, 18−25.
(56) Eaton, W. A., Munoz, V., Hagen, S. J., Jas, G. S., Lapidus, L. J., Henry, E. R., and Hofrichter, J. (2000) Fast kinetics and mechanisms in protein folding. *Annu. Rev. Biophys. Biomol. Struct. 29*, 327−359.